

Local Carrier-Based Precision Approach and Landing System

Jason T. Isaacs¹ Kenan O. Ezal² and João P. Hespanha³

Abstract—Preliminary results on the design of a precision positioning system for planes landing on an aircraft carrier in the absence of Global Positioning System (GPS) are discussed. This system relies on a set of radio transmitters similar to GPS satellite transmitters that are placed on the deck of the ship. These transmitters along with the receiver on the aircraft are fitted with specially designed antennas which allow additional directional information to be gained with each transmission. Similar to GPS, this system is capable of measuring the Pseudo-Range (PR) between the transmitter and receiver and additionally measures the Angle of Arrival (AoA) and Angle of Transmission (AoT). To achieve positioning accuracy levels necessary to autonomously land a plane on the deck of a ship requires a tight coupling of the Inertial Measurement Unit (IMU) of the aircraft and the Radio Frequency (RF) sensing designs. We present and compare two navigation filters for this application, an Unscented Kalman Filter (UKF) as well as a Nonlinear Maximum Likelihood Estimator (NLMLE). We report on extensive numerical simulations that suggest that the NLMLE approach overcomes the poor geometrical conditions of placing the transmitters on the deck of the ship to achieve the necessary accuracy levels.

I. INTRODUCTION

Toward the goal of building an accurate navigation system for planes landing on the deck of an aircraft carrier in the absence of a Global Positioning System (GPS) we wish to evaluate the accuracy of utilizing a combination of Inertial Measurement Unit (IMU), Pseudo-Range (PR), Angle of Transmission (AOT), and Angle of Arrival (AOA) measurements. In order to perform this evaluation we study the positioning accuracy of both an Unscented Kalman Filter (UKF) as well as a Nonlinear Maximum Likelihood Estimator (NLMLE) to estimate the state of an aircraft as it approaches the carrier for landing.

The objective of this work is to develop an accurate localization system to aid in the navigation of aircraft landing on the deck of an aircraft carrier in the event that GPS becomes unavailable (possibly due to jamming). By strategically placing radio transmitters on the aircraft carrier that mimic the capability of GPS satellite transmitters, one can design a navigation system that tightly integrates the radio measurements with the IMU on the aircraft to potentially

meet the accuracy requirements of the landing aircraft. A key challenge with this approach has to do with poor transmitter geometry due to space constraints on the aircraft carrier. These geometry constraints result in a large Dilution of Precision (DOP) as the receiver mounted on the landing plane gets moderately far from the transmitters mounted on the carrier. This is similar to the errors associated with a GPS position fix which only uses sensors directly overhead such as in an urban canyon setting. As a means of combatting this problem we propose using strategically designed antennas on the transmitters and receivers which allow for additional directional information to be gained from each transmitted message.

The Joint Precision Approach and Landing System (JPALS) was developed in the early 2000's to provide precise navigation support to landing aircraft in all weather conditions and visibility. The two main varieties of JPALS are the Land-based Differential GPS (LDGPS) and the Shipboard Relative GPS (SRGPS) [1]. The SRGPS relies on dual frequency carrier-phase differential GPS which relies on accurate carrier phase tracking to meet the JPALS precision requirements. Several works have been published on various aspects of JPALS [1], [2], [3], and [4]. Despite the potential benefits of including direction information including improved accuracy and reduction in number of required transmitters, there seems to have been little attention paid to this approach. Our approach seeks to use nonlinear filters to perform the sensor fusion. The first that we consider is the UKF and the second is a NLMLE. The UKF and modifications thereof have been shown to be effective in strapdown inertial navigation applications [5] and [6]. More recently as computation power has increased, numerical optimization approaches like the NLMLE are starting to become more viable for tracking and state estimation applications [7], [8], and [9].

The contributions of this work are threefold. First, we present a six-element, 12-port direction finding antenna capable of making precise AOA and AOT measurements. Second, we develop a 17 state system model which characterizes the system dynamics including position, velocity, attitude, accelerometer bias, gyroscope bias, and receiver clock bias. Finally, we numerically evaluate and compare the performance of the two nonlinear filtering techniques to fuse the additional directional information with the traditional pseudorange information.

The remainder of this paper is arranged as follows. In the next section, the problem of RF direction-finding is discussed, and a method for obtaining both AOA and AOT measurements is formalized. The system model is described

*This research was supported in part by Navy contracts N68335-14-C-0330, N68335-16-C-0104, and N14A-T009. The content of the information does not necessarily reflect the position or the policy of the Government, and no official endorsement should be inferred.

¹J.T. Isaacs is with the Department of Computer Science, California State University Channel Islands, jason.isaacs@csuci.edu

²K.O. Ezal is with Toyon Research Corporation, Goleta, CA 93117, kezal@toyon.com

³J.P. Hespanha is with Department of Electrical and Computer Engineering, University of California, Santa Barbara, hespanha@ece.ucsb.edu

in Section III. In Section IV, two navigation filters, an Unscented Kalman Filter (UKF) and a Nonlinear Maximum Likelihood Estimator (NLMLE) are described, and numerical simulations are used to compare the two filters for this application in Section V. Concluding remarks follow in Section VI.

II. RF DIRECTION-FINDING

A. Time-of-Arrival (TOA) / Pseudorange Measurements

The Global Positioning System (GPS) and other similar Global Navigation Satellite Systems (GNSS) have enabled real-time, all-weather, low-cost navigation for the masses as GNSS receivers are now embedded in virtually every mobile phone on the market today. A GNSS receiver makes use of RF emitters located on satellites to determine its own position [10]. If the orbital dynamics of satellites are known, and if the satellites are being tracked through terrestrial-based surveillance systems, the positions of the satellites relative to Earth are known. Assuming the GNSS receiver knows the time the signal was emitted (t_0), it can determine the time-of-flight (δt_i) between the receiver and satellite by recording the time-of-arrival (TOA) of the received signal (t_i) and taking the difference: $\delta t_i = t_i - t_0$. The pseudorange (ρ_i) between satellite i and the receiver at the time the signal was emitted can then be calculated as $\rho_i = c\delta t_i$, where c is the speed of light. Because the receiver and the satellite clocks are not synchronized, the receiver must measure the TOA of a least four satellite signals to determine its own 3-D location and time. While we have ignored numerous details and relativistic effects, this is the essential structure of GNSS-based navigation.

The low signal power density of GNSS signals make them vulnerable to intentional or unintentional sources of interference. While alternative sensor modalities, such as electro-optical/infrared (EO/IR) can be used for navigation, they cannot operate under all-weather conditions, including fog, rain, and sand-storms. Hence, the use of RF beacons called pseudolites has been proposed for GNSS-denied alternative navigation. Because pseudolites use the same signal structure as GNSS, receivers still require four TOA measurements for 3-D navigation.

B. Angle-of-Arrival (AOA) Measurements

The use of direction-finding (DF) measurements has the potential to reduce the number of beacons required. One DF technique is the use of angle-of-arrival (AOA) measurements to triangulate the position of the receiver relative to emitters with known positions. Figure 1 illustrates the 2-D AOA-based navigation concept where the receiver measures the direction-of-arrivals (ϕ) of received signals relative to its own coordinate system. If the emitter locations are known, then the use of three AOA measurements is sufficient to determine the receiver's 2-D position and orientation (α) without any ambiguities. Note that three TOA measurements are also sufficient to determine the 2-D position of the receiver, but are insufficient to determine its orientation. If there are only two AOA measurements, the position of the receiver can

be unambiguously determined in 2-D provided the platform orientation can be measured using some alternative measurement, such as a compass heading. However, since in the 3-D case AOA measurements include elevation (θ) as well as azimuth (ϕ), only three beacon signals are required to determine the 3-D position and orientation of the receiver. This is one less beacon than required for the TOA-only case, which cannot determine orientation.

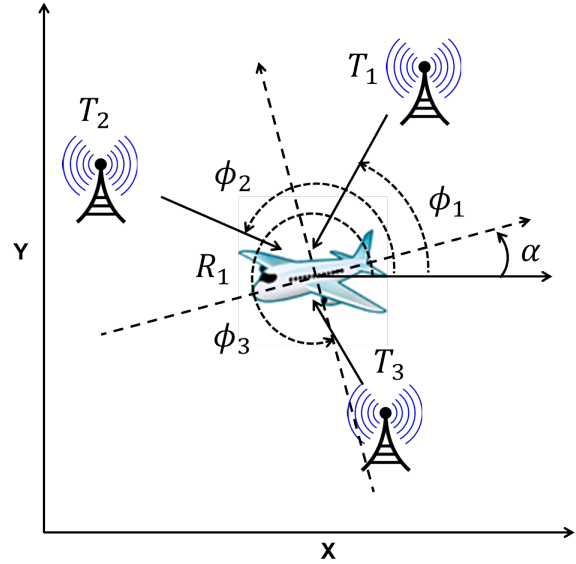


Fig. 1. Navigation with angle-of-arrival (AOA).

C. Angle-of-Transmission (AOT) Measurements

One potential downside to using AOA measurements is that the receiver and the receiver antenna are necessarily more complex. There is, however, another DF technique that we refer to as angle-of-transmission (AOT) that does not require a direction-finding antenna at the receiver. Figure 2 illustrates the navigation concept of operations for AOT measurements. In this case, the receiver measures the direction-of-transmission (ϕ) of the signal in the coordinate frame of the transmitter. As illustrated in Figure 3, if the transmitter locations and orientations are known, then only two AOT measurements are required to determine the 2-D position of the receiver. Hence, measurements θ_1 and θ_2 , together with the known distance ρ_{12} between the two transmitters, are sufficient to compute the ranges ρ_1 and ρ_2 to the receiver, and therefore the receiver position relative to the emitters. In fact, even in 3-D, two beacons are sufficient to estimate the 3-D position of the receiver, if the AOT measurement includes both elevation and azimuth (θ, ϕ) components. Note that neither AOA nor AOT measurements preclude the ability to measure the TOA, or pseudorange (ρ) to the emitter. Hence, we can devise systems that make use of TOA, AOA, and/or AOT measurements.

D. Illustrative System

The process of obtaining AOT measurements is identical to the process of obtaining AOA measurements. The only

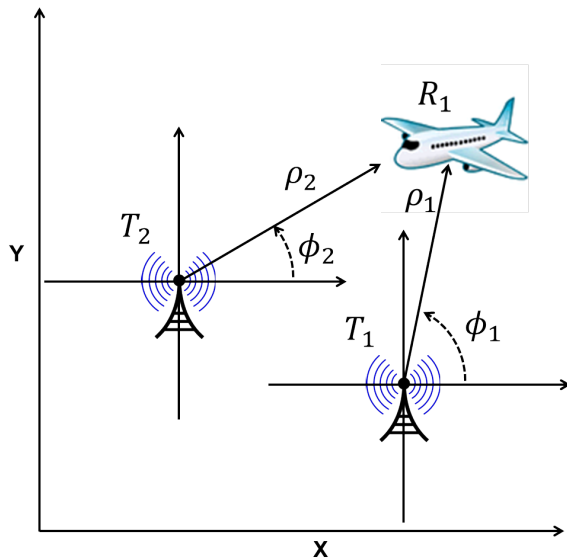


Fig. 2. Navigation with angle-of-transmission (AOT).

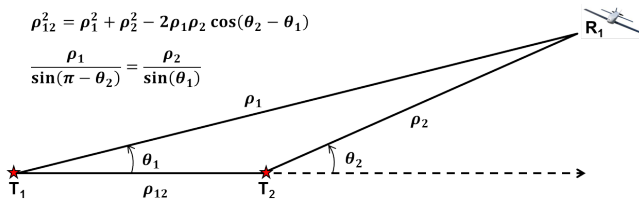
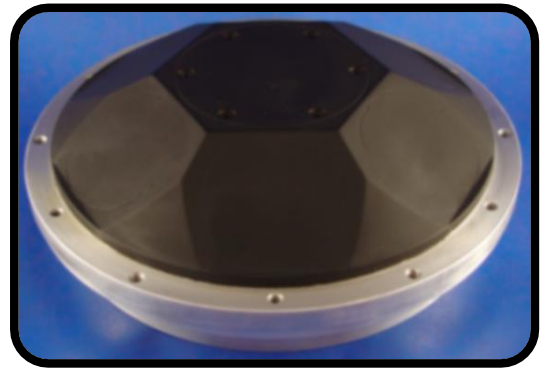


Fig. 3. AOT geometry.

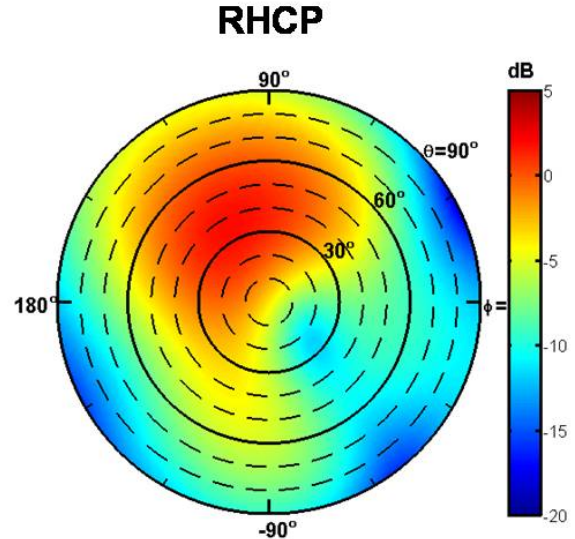
difference is where the computations are done and the number of signals that are transmitted. For example, if in Figure 2 the roles were reversed and transmitter (T_1) was the receiver, and the receiver (R_1) was the transmitter, then the angle ϕ_1 would be the angle-of-arrival as measured by T_1 's N-port DF antenna. To measure the AOA we would require knowledge of the antenna manifold $\bar{a}_{T_1}(\theta, \phi)$ and make use of a DF algorithm of our choice, such as the Multiple Signal Characterization (MUSIC) algorithm [11]. When measuring the angle-of-transmission by T_1 , the receiver R_1 requires knowledge of the antenna manifold $\bar{a}_{T_1}(\theta, \phi)$, which is defined as

$$\bar{a}_{T_1}(\theta, \phi) = [a_1(\theta, \phi) \ a_2(\theta, \phi) \ \dots \ a_N(\theta, \phi)] \quad (1)$$

where $a_k(\theta, \phi)$ is the complex gain pattern of the k th antenna port or element. In the adaptive antenna literature the manifold (1) is sometimes referred to as the steering vector. However, the receiver does not require a DF antenna itself. Instead, T_1 transmits a unique (orthogonal) waveform of equal power from each of its N antenna ports. All waveforms must be phase-locked to each other, which is easy since the same clock is used to generate all waveforms. The receiver with a single-port antenna receives all signals, and using matched filters extracts relative magnitude and phase measurements that are used to compute the AOT using the same DF algorithm that could have been used by the transmitter had the roles been reversed. As an example, Figure



(a) 5.5-in six-element, 12-port DF antenna



(b) Single-port RHCP magnitude pattern for upper hemisphere:

Fig. 4. Six-element, 12-port DF antenna.

4(a) shows a six-element circular array with dual-polarized elements having a total of 12 ports. Figure 4(b) illustrates the right-hand circularly polarized (RHCP) magnitude pattern of the first port of the antenna. Each port also has a left-hand circularly polarized (LHCP) magnitude pattern and a phase pattern that are not shown.

Figure 5 shows the cumulative DF probability of the 12-port antenna using the MUSIC algorithm with an average SNR of 30 dB. Three cases are shown: A linearly polarized (1S: LinPol) signal, a RHCP (1S: RHCP) signal, and four linearly polarized (4S: LinPol) signals. The remaining curves correspond to ideal antennas that have 0.1° , 1.0° , and 10.0° one-sigma Gaussian DF error distributions. For example, the 1S: LinPol curve indicates that 70% of the DF errors of the 12-port antenna are less than 0.3° when faced with a single linearly polarized signal. When faced with four signals, this performance drops to 0.5° . This performance holds whether the antenna is being used as a transmitter (AOT) or a receiver (AOA).

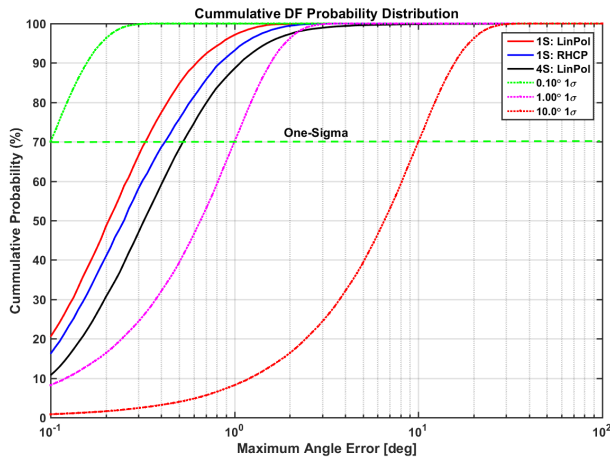


Fig. 5. Cumulative direction-finding probability.

III. SYSTEM MODEL

The main elements of this location system are the states associated with the aircraft and sensors,

$$x = [p^T \quad \dot{p}^T \quad e^T \quad a_b^T \quad \omega_b^T \quad \Delta t]^T \quad (2)$$

Where $p \in \mathbb{R}^3$ and $\dot{p} \in \mathbb{R}^3$ represent the position and velocity of the aircraft in the navigation frame, $e = [e_0 \ e_1 \ e_2 \ e_3]^T$ is the unit quaternion representing the aircraft attitude, $a_b \in \mathbb{R}^3$ is the vector representing IMU accelerometer bias, $\omega_b \in \mathbb{R}^3$ is the vector representing IMU gyro bias, and Δt is the scalar representing the receiver radio clock bias. There are M transmitters located at points, $q := [q_1 \ q_2 \ \dots \ q_n] \in \mathbb{R}^{3 \times M}$. Each transmitter broadcasts a time-stamped t_0 electro-magnetic signal, which propagates outward at speed c . A receiver on the aircraft records the time at which each transmitted signal arrives and compares these times to the timestamps to compute M pseudo-range measurements (PR). Additionally, the receiver is capable of recording the angle of arrival (AOA) and angle of transmission (AOT) of each transmitted signal. The main objective of the localization system is to track the state vector x by tightly integrating the IMU with the available PR, AOA, and AOT measurements.

A. Pseudo-Range Measurements

The pseudo-range measurement due to transmitter i is modeled as:

$$\rho_i = \|p - q_i\| + \Delta t c. \quad (3)$$

Here Δt represents the unknown clock bias of the receiver.

B. Angle of Transmission Measurements

The angle of transmission measurement due to transmitter i is taken with respect to the navigation frame and is modeled as:

$$\alpha_i = \text{atan2}(p_y - q_{iy}, p_x - q_{ix}) \quad (4)$$

$$\beta_i = \text{atan2}\left(p_z - q_{iz}, \sqrt{(p_x - q_{ix})^2 + (p_y - q_{iy})^2}\right) \quad (5)$$

Here $\text{atan2}()$ is the two argument inverse tangent function.

C. Angle of Arrival Measurements

The angle of arrival measurement due to transmitter i is taken with respect to the body frame and thus must be rotated to the navigation frame. The AOA measurement is modeled as:

$$\theta_i = \text{atan2}(\bar{v}_{iy}, \bar{v}_{ix}) \quad (6)$$

$$\phi_i = \text{atan2}\left(\bar{v}_{iz}, \sqrt{\bar{v}_{ix}^2 + \bar{v}_{iy}^2}\right) \quad (7)$$

Where \bar{v}_i is the vector pointing from the aircraft to transmitter i transformed to the body frame by rotating by e as follows,

$$v = p - q_i \quad (8)$$

$$\bar{v} = C_n^b v \quad (9)$$

where C_n^b is the rotation matrix transforming vectors in the navigation frame to the body frame as described in [5],

$$C_n^b = (C_b^n)^T \quad (10)$$

$$= 2 \begin{bmatrix} 0.5 - e_2^2 - e_3^2 & e_1 e_2 + e_0 e_3 & e_1 e_3 - e_0 e_2 \\ e_1 e_2 - e_0 e_3 & 0.5 - e_1^2 - e_3^2 & e_2 e_3 + e_0 e_1 \\ e_1 e_3 + e_0 e_2 & e_2 e_3 - e_0 e_1 & 0.5 - e_1^2 - e_2^2 \end{bmatrix} \quad (11)$$

D. Inertial Measurement Unit (IMU)

The IMU is capable of making acceleration \tilde{a} and angular-velocity $\tilde{\omega}$ measurements which are corrupted by time varying biases a_b and ω_b and zero mean additive noise terms n_a and n_ω .

E. System Dynamics

In [5], a UKF was shown to have significant advantages over an Extended Kalman Filter (EKF) for similar applications. We will follow closely the state-space model described in this work. The dynamical system we will use is:

$$x_{k+1} = f(x_k, u_k, v_k) \quad (12)$$

$$y_k = h(x_k, u_k, n_k) \quad (13)$$

where x_k represents the unobserved state vector and y_k represents the vector of observations, u_k represented the IMU measurements, and v_k and n_k represent multiplicative zero-mean Gaussian noise. The discrete time state vector is written as,

$$x_k = \begin{bmatrix} p[k] \\ \dot{p}[k] \\ e[k] \\ a_b[k] \\ \omega_b[k] \\ \Delta t[k] \end{bmatrix}. \quad (14)$$

The RF measurement vector y_k is written as,

$$y_k = \begin{bmatrix} \alpha_1[k] \\ \beta_1[k] \\ \theta_1[k] \\ \phi_1[k] \\ \rho_1[k] \\ \vdots \\ \alpha_M[k] \\ \beta_M[k] \\ \theta_M[k] \\ \phi_M[k] \\ \rho_M[k] \end{bmatrix}. \quad (15)$$

The IMU measurement vector u_k is written as,

$$u_k = \begin{bmatrix} a_x[k] \\ a_y[k] \\ a_z[k] \\ \omega_1[k] \\ \omega_2[k] \\ \omega_3[k] \end{bmatrix} \quad (16)$$

as described above. For this study we write the simplified kinematic equations of the aircraft in a reference frame relative to the ship. This kinematic model is a discrete time version of the kinematic navigation equations described in [5] which include additional terms for IMU bias errors and receiver clock error,

$$x_{k+1} = f(x_k, u_k, v_k) \quad (17)$$

$$= \begin{bmatrix} p[k] + dTv[k] + \frac{dT^2}{2}\bar{a} \\ v[k] + dT\bar{a} \\ \left[I_{3 \times 3} (\cos(s) + \eta dT\lambda) - \frac{1}{2}\Phi_\Delta \frac{\sin(s)}{s} \right] e[k] \\ a_b[k] + dTw_{ab} \\ \omega_b[k] + dTw_{\omega_b} \\ \Delta t[k] + dTw_{\Delta t} \end{bmatrix}. \quad (18)$$

where \bar{a} is treated as measured accelerations transformed into the global reference frame,

$$\bar{a} = C_b^n \left([a_x[k] a_y[k] a_z[k]]^T - a_b - n_a \right) + [0 \ 0 \ 1]^T g \quad (19)$$

and

$$\Phi_\Delta = dT \begin{bmatrix} 0 & \bar{\omega}_1 & \bar{\omega}_2 & \bar{\omega}_3 \\ -\bar{\omega}_1 & 0 & -\bar{\omega}_3 & \bar{\omega}_2 \\ -\bar{\omega}_2 & \bar{\omega}_3 & 0 & -\bar{\omega}_1 \\ -\bar{\omega}_3 & -\bar{\omega}_2 & \bar{\omega}_1 & 0 \end{bmatrix} \quad (20)$$

where,

$$\bar{\omega} = [\omega_1[k] \ \omega_2[k] \ \omega_3[k]]^T - \omega_b - n_\omega, \quad (21)$$

$$s = \frac{1}{2} \|\bar{\omega}\|, \quad (22)$$

$$\lambda = 1 - \|e[k]\|^2, \quad (23)$$

and η is a constant parameter used to ensure that $e[k]$ remains close to unit norm. The final three terms model the accelerometer, gyro, and receiver clock biases as discrete time random-walks where w_{ab} , w_{ω_b} , and $w_{\Delta t}$ are zero-mean Gaussian random variables.

IV. NAVIGATION FILTERS

The RF measurements described in Section III can be fused with an inertial measurement unit (IMU) on the aircraft in a tightly coupled navigation filter [12]. To provide the state estimation we will evaluate the performance of an Unscented Kalman Filter (UKF) as well as a Nonlinear Maximum Likelihood Estimator (NLMLE) to fuse the nonlinear measurements with predictions from state-space model.

For the UKF implementation we followed the algorithm described in Appendix A of [5]. In [5], it was demonstrated that the UKF is an effective means of fusing IMU data with position and velocity measurement provided by a GPS receiver. The key difference between this work and that of [5] is our inclusion of PR, AOA, and AOT measurement in the observation model.

The NLMLE numerically finds the trajectory that maximizes the likelihood of the measurements described in Sections III-A through III-D, assuming that all these measurements are corrupted by independent additive Gaussian noise. Because the measurement equations and the system dynamics are nonlinear, the likelihood maximization has to be carried out numerically using a nonlinear optimization engine. Specifically, we seek to find the state trajectory that satisfies the dynamics in Section III-E, while maximizing the likelihood of a window of past measurements, which is proportional to an appropriately defined sum of squared errors. Such an estimator is often also called a Minimum Energy Estimator [7] or Moving Horizon Estimation [13]. The numerical optimization was carried out using a fast solver, developed especially for this application. For more information on the implementation of the NLMLE filter the reader is referred to the following tech reports [14] and [15].

V. NUMERICAL SIMULATION

A. Parameters and Test Description

The test setup involved placing five transmitters on the deck near the stern of the carrier. The origin of this coordinate system is the point where the aircraft touches down on the carrier. The sensor locations in this coordinate system (units of meters) are $(-80, 20, 0)$, $(-80, -20, 0)$, $(0, 36, 0)$, $(0, -36, 0)$, and a fifth sensor is assumed to be placed in the tower at $(-36, 20, 40)$. The aircraft trajectory for the test is starting at around 1 mile from the touch down point at an altitude of 100 meters (3.5 degree glide slope). The sample rate of the IMU is set to 25 Hz, and the sample rate of the radio based measurements was set to 5 Hz. One hundred Monte Carlo trials were performed to evaluate the accuracy benefits including the extra AOA and AOT measurements that may be obtained by using appropriately designed directional antennas. Here the initial state estimate was corrupted with additive noise for position, velocity, and

TABLE I
SIMULATION PARAMETERS

Radio Measurement Noise	
AOA - σ_{n_k}	$1 (\pi/180)$
AOT - σ_{n_k}	$1 (\pi/180)$
PR - σ_{n_k}	$1/2$
IMU Measurement Noise	
$a_b(0)$	0.02
$\omega_b(0)$	$1 (\pi/180) (1/3600)$
σ_{n_a}	$4e^{-4}$
σ_{n_ω}	$0.01 (\pi/180) (1/60)$
$\sigma_{w_{\omega b}}$	$1 (\pi/180) (1/3600) (1/60)$
$\sigma_{w_{ab}}$	$2e^{-4}$
Receiver Clock Noise	
$\Delta t(0)$	$30/c$
$\sigma_{w_{\Delta t}}$	$3e^{-5}/c$

attitude. The parameters for the Monte Carlo Simulations can be found in Table I.

B. Simulation Results

The estimate trajectories were logged for 100 Monte Carlo trials for both the UKF and the NLMLE. While the UKF performs satisfactory in the critical area near landing zone, the estimate is biased and results in a very large mean squared error (MSE) in the far-field away from the ship. This can be seen in Figure 6 which has been cropped to errors less than $100 m^2$ to show detail near the ship. In this figure the plane touches down on the deck of the carrier at 35 seconds into the simulation. The NLMLE however is not biased and in fact performs quite well in both the far-field and near the ship as can be seen from Figure 8.

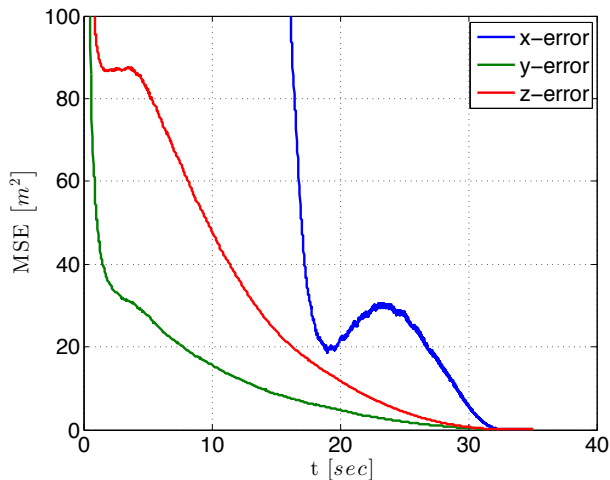
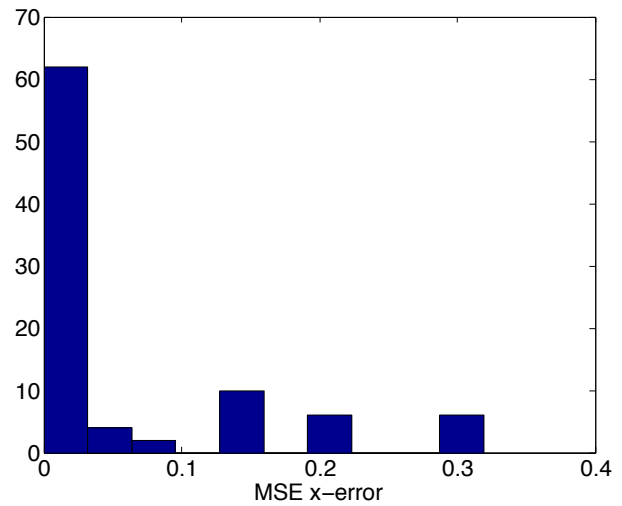
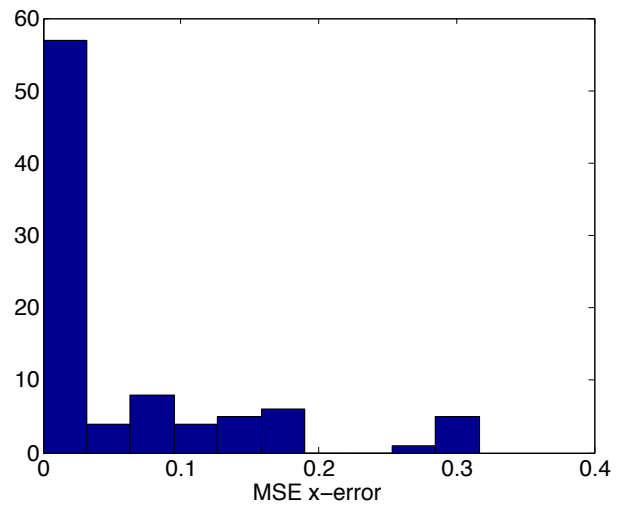


Fig. 6. MSE in x, y, and z directions for UKF.

While the UKF estimate is biased and quite large in the far-field the estimate is less noisy than the estimate provided by the NLMLE. This can be better visualized by looking at a histogram of the errors at a particular time-stamp in the trajectory across all runs. Figure 7, shows a histogram of the MSE in the x-direction for both the UKF and NLMLE just a few meters from the edge of the ship. As you can see, the



(a) MSE x-component for the NLMLE near the ship.



(b) MSE x-component for UKF near the ship.

Fig. 7. MSE in x direction for NLMLE and UKF near the ship.

accuracy is essentially the same with both methods achieving a high level of accuracy.

VI. CONCLUSIONS

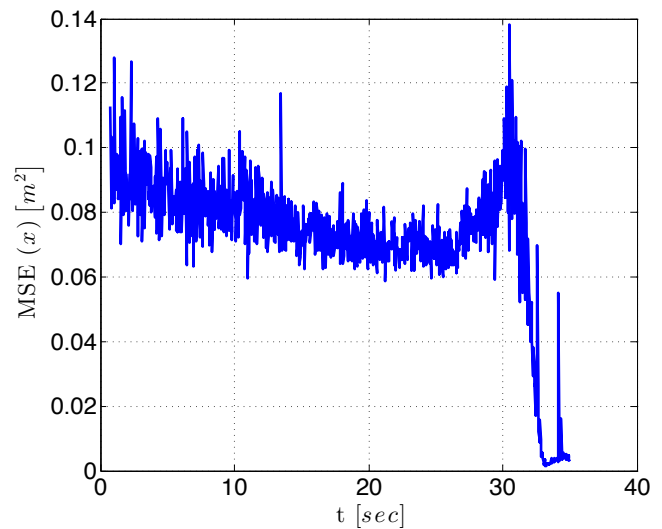
We have proposed a system model for a shipboard relative navigation system capable of providing a complete navigation solution for aircraft in the act of landing on an aircraft carrier. This system model includes fusing acceleration and angular velocity information from the IMU onboard the aircraft, traditional pseudorange measurements similar to GPS using pseudolites mounted on the deck of the aircraft carrier, and measurements obtained through RF direction finding techniques. Two different data fusion techniques were evaluated for this application. While the UKF was shown to meet the positioning accuracy requirements near the ship, the solution had the undesirable property of providing a biased estimate. This was particularly noticeable far from the ship. The NLMLE approach produced an unbiased estimate and provided a more accurate overall estimate. The one drawback to the NLMLE method is that it requires numerical

optimization techniques to solve for the estimate. Therefore the UKF could always be running in parallel in order to both provide a warm start to the numerical optimization as well as a fallback plan in case the optimization does not converge to a solution.

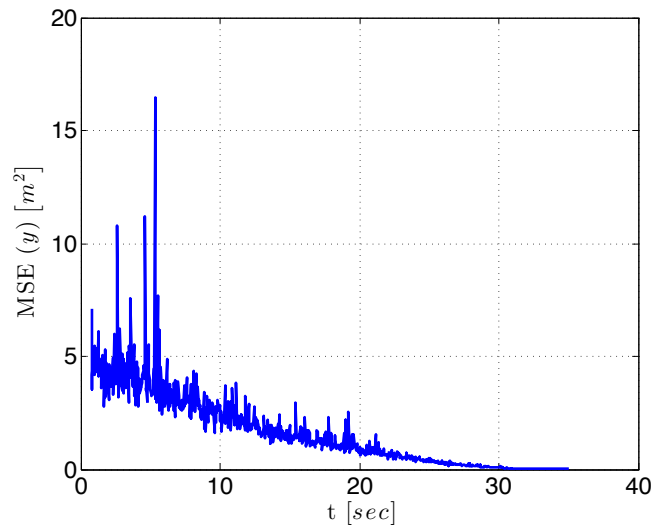
There are several directions in which this work may be extended. The next step will be to build a prototype system to act as a test platform for further algorithm development. We plan to initially run experiments on a ground vehicle and then proceed to a manned aircraft. The numerical optimization for the NLMLE was carried out using a fast solver, developed especially for this project. We continue to seek ways to improve the performance and robustness of this solver. Finally, the system presented here could potentially be modified to provide precise navigation for self-driving cars in urban canyon environments where GPS accuracy suffers due to signal blockage.

REFERENCES

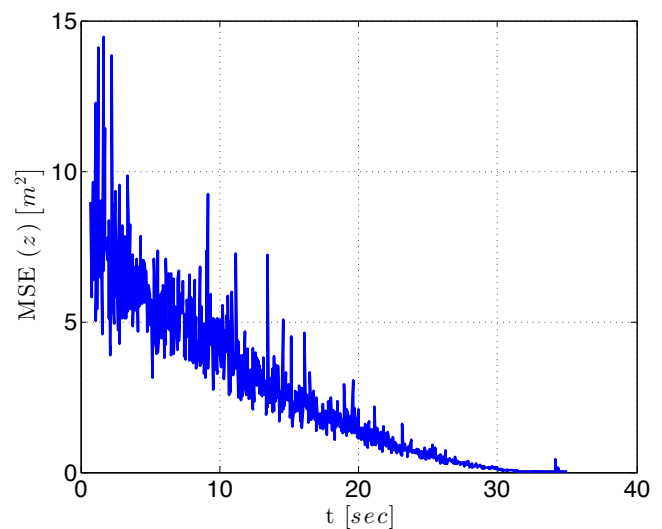
- [1] U. S. Kim, D. S. De Lorenzo, D. Akos, J. Gautier, P. Enge, and J. Orr, "Precise phase calibration of a controlled reception pattern GPS antenna for JPALS," in *Position Location and Navigation Symposium, PLANS*. IEEE, 2004, pp. 478–485.
- [2] D. S. De Lorenzo, J. Gautier, and P. Enge, "GPS attitude determination for a JPALS testbed: integer initialization and testing," in *Position Location and Navigation Symposium, PLANS*. IEEE, 2004, pp. 762–770.
- [3] S. Dogra, J. Wright, and J. Hansen, "Sea-based JPALS relative navigation algorithm development," in *Proceedings of the 18th International Technical Meeting of the Satellite Division of the Institute of Navigation ION GNSS*, 2005, p. 2871.
- [4] A. Brown and B. Mathews, "A robust GPS/INS kinematic integrity algorithm for aircraft landing," in *Proceedings of ION GNSS*, 2006.
- [5] R. Van Der Merwe, E. A. Wan, and S. Julier, "Sigma-point Kalman filters for nonlinear estimation and sensor-fusion: Applications to integrated navigation," in *Proceedings of the AIAA Guidance, Navigation & Control Conference*, 2004.
- [6] H. Hu and X. Huang, "SINS/CNS/GPS integrated navigation algorithm based on UKF," *Journal of Systems Engineering and Electronics*, vol. 21, no. 1, pp. 102–109, 2010.
- [7] A. P. Aguiar and J. P. Hespanha, "Minimum-energy state estimation for systems with perspective outputs," *IEEE Transactions on Automatic Control*, vol. 51, no. 2, pp. 226–241, 2006.
- [8] L. R. G. Carrillo, W. J. Russell, J. P. Hespanha, and G. E. Collins, "State estimation of multiagent systems under impulsive noise and disturbances," *IEEE Transactions on Control Systems Technology*, vol. 23, no. 1, pp. 13–26, 2015.
- [9] S. A. Quintero, D. A. Copp, and J. P. Hespanha, "Robust UAV coordination for target tracking using output-feedback model predictive control with moving horizon estimation," in *American Control Conference (ACC)*. IEEE, 2015, pp. 3758–3764.
- [10] E. Kaplan and C. Hegarty, *Understanding GPS: principles and applications*. Artech house, 2005.
- [11] R. O. Schmidt, "A signal subspace approach to multiple emitter location spectral estimation," Ph.D. dissertation, Stanford University, 1981.
- [12] D. Titterton and J. L. Weston, *Strapdown inertial navigation technology*. IET, 2004, vol. 17.
- [13] D. A. Copp and J. P. Hespanha, "Nonlinear output-feedback model predictive control with moving horizon estimation," in *53rd Annual Conference on Decision and Control (CDC)*. IEEE, 2014, pp. 3511–3517.
- [14] —, "Nonlinear output-feedback model predictive control with moving horizon estimation: Illustrative examples," University of California, Santa Barbara, Santa Barbara, Tech. Rep., Oct. 2015.
- [15] D. Copp and J. P. Hespanha, "Nonlinear output-feedback model predictive control with moving horizon estimation," University of California, Santa Barbara, Santa Barbara, Tech. Rep., May 2014.



(a) MSE x-component



(b) MSE y-component



(c) MSE z-component

Fig. 8. MSE in x, y, and z directions for NLMLE.